Resource-Efficient Technologies 3 (2017) 177–186

Contents lists available at ScienceDirect

Resource-Efficient Technologies

journal homepage: www.elsevier.com/locate/reffit

Research paper

Pressurized hot water extraction of 10-deacetylbaccatin III from yew for industrial application ☆

Maximilian Sixt, Jochen Strube*

Institute for Separation and Process Technology, Clausthal University of Technology, 38678 Clausthal-Zellerfeld, Germany

ARTICLE INFO

Article history:
Received 31 October 2016
Revised 24 March 2017
Accepted 27 March 2017
Available online 17 May 2017

Keywords:
Green solvents
Pressurized hot water extraction
Modeling
Yew
Simulation
Process design
PHWE

ABSTRACT

In this study a systematic and model-based approach for a process development focusing on pressurized hot water extraction (PHWE) is investigated, considering potential thermal degradation of high-value compounds. For extraction of 10-deacetylbaccatin III (10-DAB) from yew as a representative test system, water at 120 °C provided the best compromise between extraction yield and thermal degradation. A yield of almost 100% with regard to the overall amount of 10-DAB was reached in only 20 min. Each experiment for model parameter determination was carried out with 1.9 g of plant material at a flowrate of 1 mL/min and an applied pressure of 11 bar. All experimental values are assessed by a physico-chemical (rigorous) extraction model with experimental values and simulation results showing high conformity. In order to demonstrate the usability of the extraction model and model parameter determination a scale-up prediction was calculated. The scale-up experiments were predicted precisely and thus the model validated. The experiments and the simulation results for a column with a volume of 104 mL and a mass of 22 g yew needles were consistent with the milli-scale used for model parameter determination.

1. Introduction

The extraction of valuable compounds from plant material is mainly performed with conventional organic solvents. Many of these solvents have unwanted aspects like flammability, volatility, toxicity, and jointly contribute to environmental pollution and the greenhouse effect. Moreover, it must be proven that residuals of these solvents in the extracts cause no health risk when consumed, for example as pharmaceuticals [1]. These drawbacks call for alternative solvents and processes. Various methods have been published in terms of “Green Extraction” [1] to reduce or even avoid conventional solvents. Both et al. described the extraction of polyphenols from black tea with the aid of ultrasound [2]. Another alternative solvent is supercritical CO_2 which is already state of the art for the extraction of hop and coffee [3]. Further alternative solvents, like δ-limonene, ionic liquids or agro-solvents like ethanol can be found in recent publications [4–7].

Another alternative green solvent is water, which will be the focus of this work. Its window of polarity and thereby its solubilization potential can be substantially increased, if water is used under high temperature and pressure as a solvent for phytoextraction.

2. Materials and methods

2.1. General principles

In pressurized hot water extraction (PHWE), the extraction of valuable compounds from plants is carried out with water in the temperature range above its atmospheric boiling point but below the critical point. Water’s polarity is typically quantified by the dielectric constant ε, which however can be changed over an extremely wide range by varying temperature. Under ambient conditions ε of water has a value of roughly 80, decreasing to 34.8 at 200 °C, thus being close to the value of methanol (32.7) at ambient conditions [8,9]. The corresponding dielectric constant of various organic solvents under normal conditions and the data for water are given in Fig. 1.

The dielectric constant of water can be calculated by equation (1) [10].

☆ Peer review under responsibility of Tomsk Polytechnic University.

* Corresponding author. Institute for Separation and Process Technology, Clausthal University of Technology, 38678 Clausthal-Zellerfeld, Germany.
Tel.: +495323722355; fax: +49 5323 72 3570.
E-mail address: strube@itv.tu-clausthal.de (J. Strube).

http://dx.doi.org/10.1016/j.reffit.2017.03.007

Nomenclature

A	parameter for equation (1), m^3/kg
a_P	specific surface area, 1/m
B	parameter for equation (1), m^6/kg^2
C	parameter for equation (1), m^6/kg^2
c_L	concentration in the liquid phase, kg/m^3
c_P	concentration in the porous particle, kg/m^3
c_v	concentration in a specific vessel, kg/m^3
D	parameter for equation (1), m^6/kg^2
D_{ax}	axial dispersion coefficient, m/s^2
D_{eff}	effective diffusion coefficient, m^2/s
E	parameter for equation (1), m^6/kg^3
F	parameter for equation (1), m^6/kg^3
G	parameter for equation (1), m^6/kg^3
H	parameter for equation (1), m^8/kg^4
I	parameter for equation (1), m^8/kg^4
K	parameter for equation (1), m^8/kg^4
k	reaction rate coefficient, depending on order of reaction
K_L	equilibrium constant, m^3/kg
k_{EC}	rate coefficient in the extraction column, depending on order of reaction
k_f	mass transport coefficient, m/s
k_{SV}	rate coefficient in the storage vessel, depending on order of reaction
n	order of reaction, –
Pe	Péclet number
q	loading, kg/m^3
q_{max}	maximum loading, kg/m^3
Re	Reynolds number
r	radius, m
Sc	Schmidt number
Sh	Sherwood number
T	temperature, K
t	time, s
T^*	normalized temperature for equation (1), –
u_z	superficial velocity, m/s
V	volume, m^3
$\dot{V}$	volume flow, m^3/s
z	coordinate in axial direction, m
ε	dielectric constant, –
ε	voids fraction, –
ρ	density, kg/m^3
ρ^*	normalized density for equation (1), –
τ_{EC}	residence time in the extraction vessel, s
τ_{SV}	residence time in the storage vessel, s

Abbreviations

10-DAB	10-deacetylbaccatin III
RP-HPLC	reversed phase high performance liquid chromatography
DAD	diode array detector
DPF	distributed plug flow
i.d.	inner diameter
PEEK	polyether ether ketone
PHWE	pressurized hot water extraction
rpm	revolutions per minute

$$\varepsilon = 1 + \left(\frac{A}{T*}\right)\rho* + \left(\frac{B}{T*} + C + DT*\right)\rho*^2 + \left(\frac{E}{T*} + FT* + GT*^2\right)\rho*^3 + \left(\frac{H}{T*^2} + \frac{I}{T*} + K\right)\rho*^4 \quad (1)$$

$$T* = \frac{T}{298.15K}$$

$$\rho* = \frac{\rho}{1000kg/m^3}$$

$A = +7.62571$

$B = +244.003$

$C = -140.569$

$D = +27.7841$

$E = -96.2805$

$F = +41.7907$

$G = -10.2099$

$H = -45.2059$

$I = +84.6395$

$K = -35.8644$

Besides the dielectric constant of water, some other parameters are affected by temperature increase. For example the pH, which is 7 at normal conditions, changes to a value of 5.5 at 250 °C. Some other highly temperature-sensitive parameters are the surface tension, self-diffusivity and viscosity [9].

In recent publications the pressurized hot water extraction was investigated for the extraction of phenolic compounds, lignans, carotenoids, oils, lipids, essential oils and other bioactive compounds [11]. Rodriguez-Meizoso et al. [12] described the extraction of nutraceuticals from oregano leaves. The highest antioxidant activity and yield were achieved at a temperature of 200 °C. Optimized extraction conditions using water at 200 °C and 200 bar with an overall extraction time of 30 min were found by Bajer et al. for extraction of capsaicinoids from chilies [13]. The results showed a higher yield and productivity compared to Soxhlet extraction with pure methanol. Vázquez et al. [14] optimized the extraction conditions for anthraquinones from cegadera, which show antibacterial, antiviral, and anticancer activity. A temperature of 170 °C was found to give the best results. At higher temperatures the yield decreases due to thermal decomposition. Different areas of application for PHWE like the extraction of plants and food materials, the analysis of organic contaminants in food, extraction of pesticides and herbicides in soils and the treatment of environmental samples for analytical purpose like brominated flame retardants are listed by Teo [15].

2.2. Experimental setup

2.2.1. Milli-scale device for extraction experiments

The flow diagram of the PHWE equipment for batch extraction experiments is shown in Fig. 2. The water is pumped from a storage vessel with a HPLC pump P130 from VWR® to the extraction column filled with ground plant material. The extraction column is made from stainless steel with 10 mm i.d. × 100 mm (approx. 7.85 mL). The column itself and a coil made of a steel capillary (length = 3 m, i.d. = 1 mm) are placed in a GC oven HP 5890 Series II Plus serving as heating device. The water is preheated in the coil before reaching the extraction column. The extract leaves the extraction column at the back-end where a filter frit serves for solid–liquid separation. The extract is transferred into a second coil for effective cooling (length = 3 m, i.d. = 1 mm). The pressure drop is adjusted to 11 bar with a valve to keep the water in the liquid state.

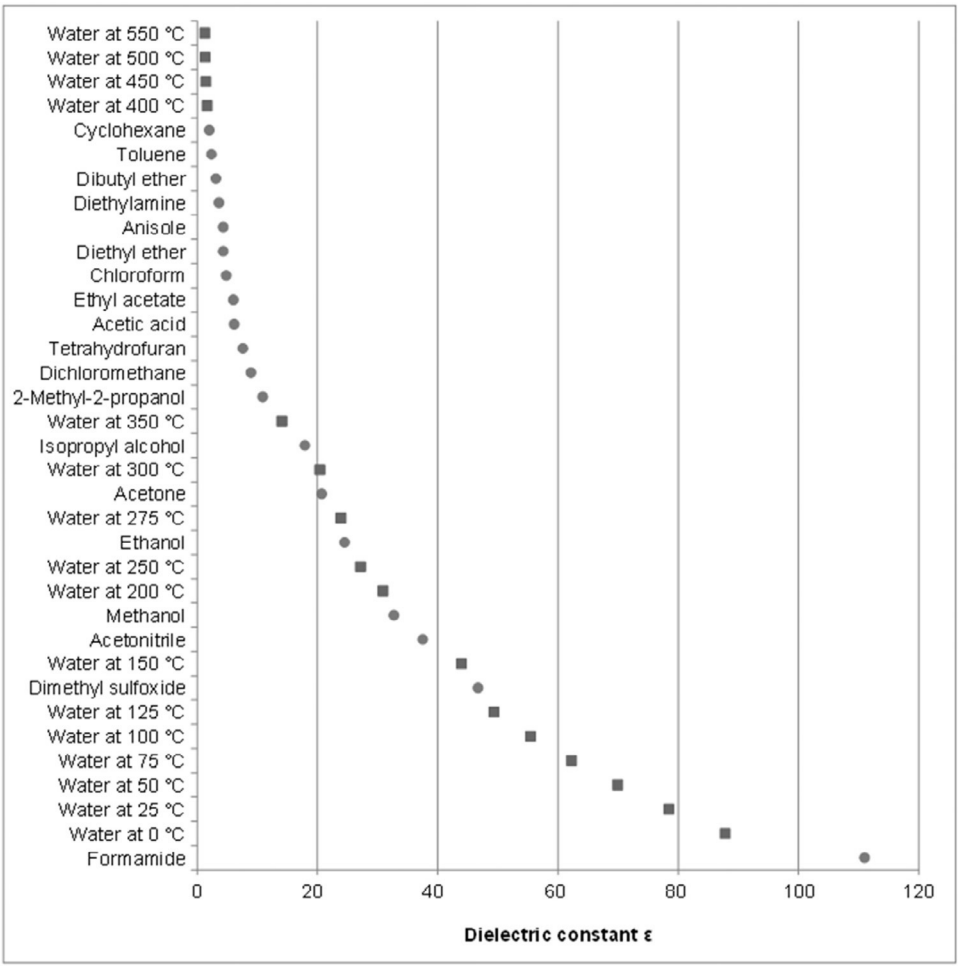

Fig. 1. Dielectric constant chart, values from Ref. [8] and equation (1).

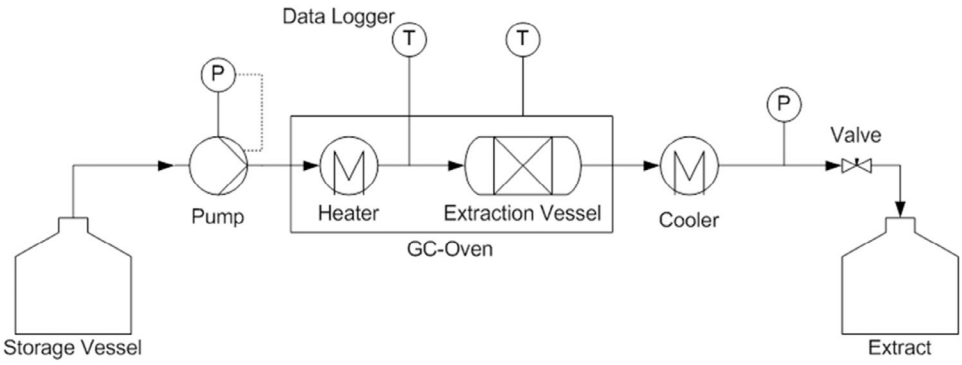

Fig. 2. Flow diagram of the milli-scale PHWE equipment for batch extraction experiments.

2.2.2. Milli-scale device for determination of thermal degradation

To determine the thermal degradation of the investigated components during extraction, the milli-scale device is modified to operate in recycling mode. This setup is shown in Fig. 3. The extract is transferred into the storage vessel (max. 100 mL) and is recycled during the whole process. Thus the target component accumulates in the system and occurring degradation effects can be studied. The storage vessel itself is located in an ultrasonic bath for mixing and avoiding possible agglomerates as well as concentration gradients inside the vessel.

2.2.3. Lab-scale device

The flow diagram of the lab-scale device is shown in Fig. 4. The water is pumped with a HPLC Pump P130 from VWR into a heater. The heater consists of a coiled steel capillary with a length of 6 m and an inner diameter of 1 mm. This coil is located in an oil-bath heated by an IKA® Ret basic heating plate. The water's temperature leaving the heater is measured and monitored. Following the heater the water stream can be split by a two-way valve. One flow leads directly into a cooler and through a valve into waste. This option serves as a bypass while adjusting the heater in order to

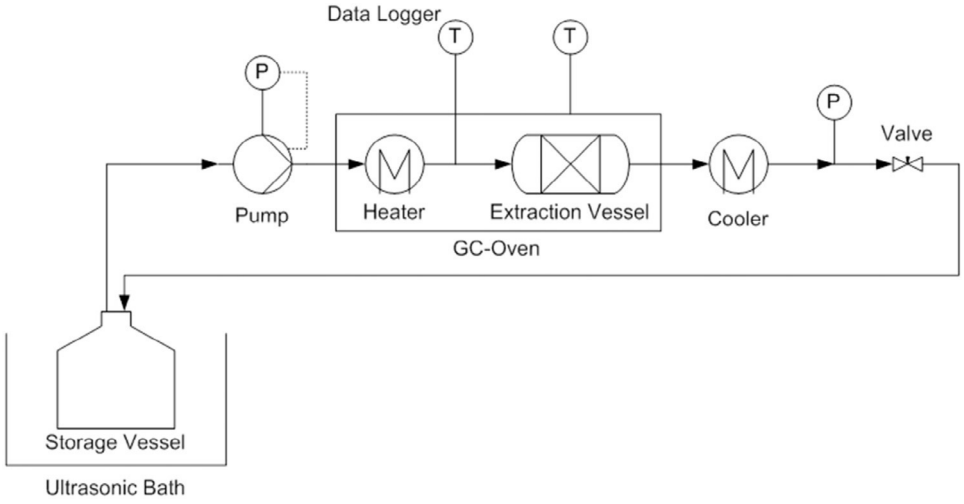

Fig. 3. Flow diagram of the milli-scale PHWE equipment in recycling mode.

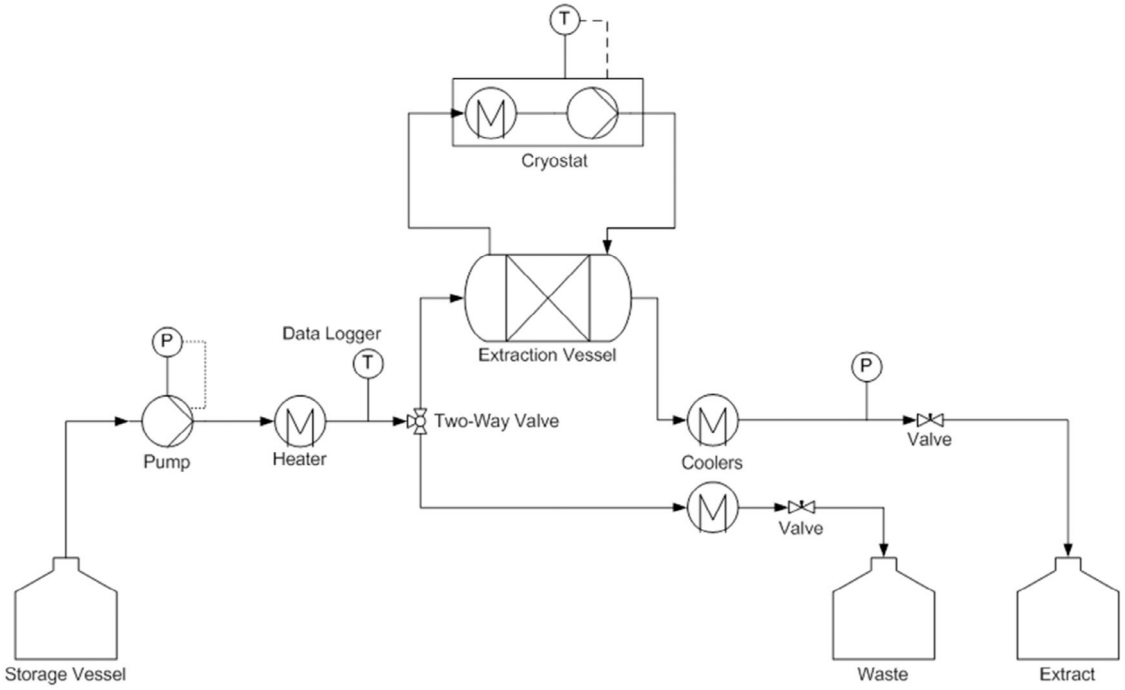

Fig. 4. Flow diagram of the lab-scale PHWE equipment.

ensure a constant temperature of the water at the desired flow. Once the water temperature is constant, the two-way valve is switched to the extraction column. The column is made of stainless steel with 24 mm i.d. × 230 mm (approx. 104 mL). Just like in the milli-scale device, filter frits provide the solid–liquid separation. Through a double jacket the column is heated by an oil-filled cryostat from Lauda®. The extract leaving the column is cooled by a coiled steel capillary (length = 6 m, i.d. = 1 mm) and passes a valve to reach a pressure drop comparable to the milli-scale device. The processed extract is stored in a vessel.

2.3. Plant material

In this work yew needles serve as a representative test system which is commonly used in the institute [16]. The needles were ordered from CfM Oskar Tropitzsch, Marktredwitz Germany. From yew, 10-deacetylbaccatin III can be obtained, serving as a precursor for the anti-cancer drug Paclitaxel® [17]. The yew needles are air dried and have a residual moisture of about 8 wt.-% and are stored in a cooling chamber at 8 °C prior to extraction. To maximize the mass transfer area during PHWE the needles are grinded in a knife mill Retsch® Grindomix GM 200 for 4 s at 4000 rpm. The particulates are classified with sieves to determine the mean particle diameter (x_{50} = 1 mm) needed for proper modeling and also to avoid dust formation which could block the frits of the extraction columns and increase back pressure.

To calculate the yield of extraction the total amount of 10-DAB $m_{10DAB,\,total}$ in the yew needles was determined a priori by conventional exhaustive solvent extraction in percolation mode. The procedure is described in detail in [16,18].

$$\text{Yield} = \frac{m_{10DAB,extracted}}{m_{10DAB,total}} \quad (2)$$

The total amount of 10-DAB referred to dry mass was 0.183% ± 0.013% (standard deviation).

2.4. Analytics

The 10-DAB in the liquid extract is analyzed with an Elite La Chrom® HPLC using a diode array detector DAD-L 2455 from Hitachi® and a Merck® PharmPrep P100 RP-18 250 × 4 mm analytical column. The samples are filtered through a 0.2 µm syringe filter and injected undiluted into the HPLC. The calibration is carried out with an external standard. The pure 10-DAB is ordered from Sigma-Aldrich. The samples were analyzed right after extraction to avoid any influence of storage. The method for analysis was already published by the authors [16,18,19].

3. Theory and calculations

In general, solid–liquid extraction is described by several partial models. The corresponding equations and assumptions can be found in detail in the literature. The simplest models are black-box/statistical models followed by short-cut models including separation factors and stage efficiency as a lumped factor of all non-idealities. Both approaches are not predictive and therefore not scale-able. Rigorous (or physico-chemical) models separate the different effects of the mass balance including fluid dynamics, phase equilibrium, mass transfer, as well as an energy balance. This allows prediction, even in scale, because according to theory only fluid dynamics and energy balance should differ in scale. Moreover, it allows in laboratory scale with minimal material amounts the experimental determination of the phase equilibrium which is not available for complex molecules and mixtures in data bases and of the relevant mass transfer coefficients if the fluid dynamics (and energy balance) of the scaled-down equipment is well described and taken into account [18,20,21].

In the following, only a brief overview of the model is given. In addition, relevant adaptations to predict PHWE are highlighted. The parameter determination will be shown in detail in this paper.

Because all devices used in this study were operated in percolation mode, the mass balance in the liquid phase is described by the distributed plug flow model (DPF). It serves for modeling the macroscopic mass transport in the extraction column. For the solid phase a pore diffusion model describes the mass transport in the plant material's pores. The raw material's residual load of target components and the corresponding extract's concentration are accounted for by equilibrium curves.

The target component's mass balance in the fluid phase (eq. (3)) considers accumulation, axial dispersion, convective mass transport and mass transfer from the plant material's pores into the bulk phase.

$$\frac{\partial c_L(z,t)}{\partial t} = D_{ax}\cdot\frac{\partial^2 c_L(z,t)}{\partial z^2} - \frac{u_z}{\varepsilon}\cdot\frac{\partial c_L\ (z,t)}{\partial z} - \frac{1-\varepsilon}{\varepsilon}\cdot k_f\cdot a_P\cdot[c_L(z,t) - c_P\ (r,z,t)] - k\cdot c_L^n \quad (3)$$

The axial dispersion coefficient D_{ax} describes the non-ideality of the flux in the tubular extraction vessel and is derived by correlations using the Reynolds and Péclet number.

$$Re = \frac{u_z d_P \rho_L}{\eta\varepsilon} \quad (4)$$

For the calculation of the Reynolds number the empty tube velocity u_z has to be calculated with regard to the continuity condition. The mean particle diameter d_P is measured by sieve analysis. The solvent density as well as the viscosity can be found in common table values [22,23]. The porosity of the packed bed can be measured by tracer experiments, which are routine engineering practice, e.g. in chromatography.

$$Pe = \frac{0.2}{\varepsilon} + \frac{0.011}{\varepsilon}(\varepsilon Re)^{0.48} \quad (5)$$

Thereafter, the Péclet number is calculated by the correlation of Chung [24]. Finally equation (6) provides the value of D_{ax}.

$$D_{ax} = \frac{d_P u_z}{\varepsilon Pe} \quad (6)$$

Mass transfer from the particle into the bulk phase is calculated using the mass transfer coefficient k_f and the specific particle surface a_P. The specific surface area a_P is calculated with equation (7).

$$a_P = \frac{6}{d_P} \quad (7)$$

The mass transfer coefficient k_f is derived by correlations that are widely used in chromatography and were already applied successfully for solid–liquid extraction [16].

$$Sc = \frac{\eta}{\rho_L\cdot D_{12}} \quad (8)$$

$$Sh = \frac{k_f\cdot d_P}{D_{12}} \quad (9)$$

$$Sh = 2 + 1.1\cdot Sc^{0.33}\cdot Re^{0.6} \quad (10)$$

In addition to the distributed plug flow model, a degradation kinetic is introduced to describe the thermal decomposition of the investigated components. The rate constant k and the exponent n are measured by recycling the extract continuously which will be described in detail in the ongoing sections of this article. Typically an Arrhenius equation takes into account the dependency on temperature.

Under the assumption of spherical particulates, the following equation can be derived as a mass balance for the target component in the plant material. The effective diffusion coefficient D_{eff} has to be measured by real extraction experiments.

$$\frac{\partial q(z,r,t)}{\partial t} = D_{eff}\ (r)\cdot\left(\frac{\partial^2 c_P\ (z,r,t)}{\partial r^2} + \frac{2}{r}\cdot\frac{\partial c_P\ (z,r,t)}{\partial r}\right) + \frac{\partial D_{eff}\ (r)}{\partial r}\cdot\frac{\partial c_P\ (z,r,t)}{\partial r} \quad (11)$$

The adsorption/desorption equilibrium inside the pores is described through equilibrium curves. Herein q is the plant material's residual load linking the equilibrium curve with the pore diffusion model. A well-known approach is e.g. the Langmuir-equilibrium. The parameters K_L and q_{max} can be derived from measurements. The maximum load q_{max} is the total amount of 10-DAB introduced in section 2.3.

$$q = q_{max}\cdot\frac{K_L\cdot c}{1 + K_L\cdot c} \quad (12)$$

In recycling mode, equation (13) is used to describe the mass balance for the storage vessel. In equation (13) V is the vessel's volume, $\dot{V}$ the flux, c_L the concentration at the extraction column outlet and c_V the concentration of the target component inside the vessel itself.

$$V\cdot\frac{\partial c_V}{\partial t} = \dot{V}\cdot(c_L - c_V) \quad (13)$$

The equation is needed, because in recycling mode the concentration c_L of the target component in the fluid entering the extraction column is not zero as in the case in the normal extraction mode, because the fluid is pre-loaded. For batch extraction, equation (13) is not taken into account because fresh solvent is applied.

4. Results

The aim of this work is to perform the model parameter determination in the milli-scale device with the smallest amount of plant material possible. Subsequently, the degradation kinetic

needs to be adapted from the recycling mode to the simulation of the actual extraction. To show the usefulness of the model and the parameter determination, scale-up experiments are performed and simulated. The experimental pathway is as follows:

1 Run a screening of temperature in batch extraction experiments using the milli-scale device.
2 Measuring and calculation of the degradation kinetics in the recycling mode of the milli-scale device.
3 Simulation of the extraction curves based on batch extractions performed in milli-scale.
4 Simulation and experimental validation of the scale-up with the lab-scale device.

4.1. Experiments

Several experiments were carried out to investigate the effect of temperature increase on degradation of the target component and the overall extraction kinetics. The investigated temperature levels for determining the degradation kinetics were ambient temperature, 120 °C, 140 °C and 180 °C. The scale-up experiments were carried out by keeping the residence time in the extraction column constant. Thus 22 g of yew needles are used, the flux is 15 mL/min at ambient temperature and 120 °C. Because 10-DAB is a precursor for the semi-synthesis of cancer drugs, a purification pathway follows the extraction anyway, thus the extraction itself only has to be optimized to highest possible yield and productivity for a cost- and resource-efficient overall process design [16]. Purification is achieved during the following process steps such as liquid–liquid extraction and chromatography. Therefore only yields are considered as optimization criteria in this paper.

Remark. Every experiment is performed in triplicates. In the following the graphs show the mean values as data points. The drawn lines only serve for a better visualization! The error bars represent the standard deviation of the measurements. If no error bars are visible they are within the symbol size of the individual data points.

4.1.1. Extraction

The basic influence of temperature during PHWE is investigated by batch extraction experiments at ambient temperature, 120 °C, and 180 °C in milli-scale. The results are plotted in Fig. 5.

10-DAB was almost completely extracted after 55 min. at ambient temperature. It is remarkable that the predominant non-polar molecule 10-DAB can be extracted with polar water. Similar results are already described in literature and can be traced to natural solubilizers contained in the yew needles [16]. By increasing the temperature to 120 °C an almost complete leaching was achieved within 15 min. Thus the productivity of the extraction is more than three times higher. A further increase in temperature leads to a yield of only about 78%. Obviously, thermal degradation takes place, which will be investigated in detail in the following. Please note that in this case extraction takes place in the percolation mode by applying fresh solvent, so there are no equilibrium limitations, and 100% yield is possible.

4.1.2. Thermal degradation

Thermal degradation of the target compound is investigated with the milli-scale device in recycling mode. Samples are taken directly from the storage vessel. The results are shown in Fig. 6.

At ambient temperature an equilibrium yield of about 77% is reached after 120 min. An equilibrium is reached, because in comparison with the experiments depicted in Fig. 5 the extract is continuously recycled, thus no fresh solvent is supplied, and no exhaustive extraction is possible. By applying higher temperature, the extraction kinetics become significantly faster. At 120 °C an equilibrium yield of about 77% is reached after 20 min, thus being 6 times faster compared to extractions carried out at ambient temperature. After about 20 min however, obviously degradation occurs and yield drops to 20% after 240 min of extraction time. This trend amplifies with higher temperature. At 180 °C almost no target component can be detected after only 120 min. The degradation kinetics are linearized to derive the rate constant and the order of the reaction for proper modeling. The resulting values are shown in Table 1.

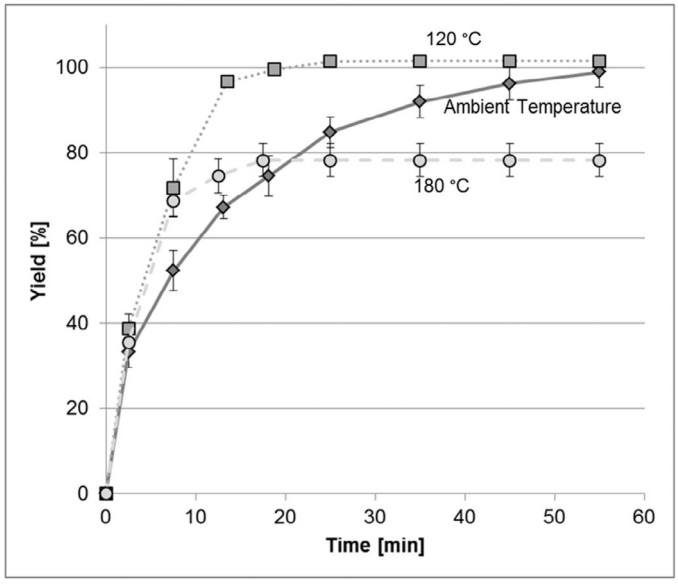

Fig. 5. Results of batch extraction with different temperatures.

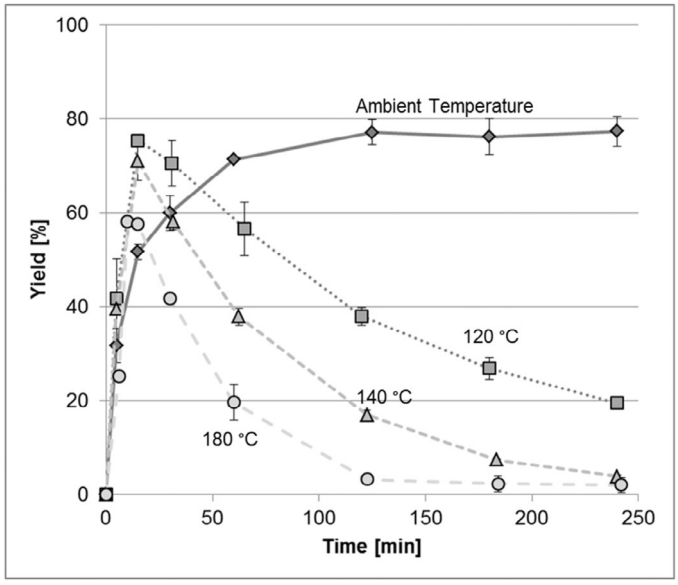

Fig. 6. Results of thermal degradation experiments at different temperature levels.

Table 1
Rate constants and orders of reaction (h = hour, g = gram, L = liter).

120 °C	140 °C	180 °C
$k = 0.8928 \cdot \frac{1}{h} \cdot \left(\frac{L}{g}\right)^{0.1627}$	$k = 0.6624 \cdot \frac{1}{h} \cdot \left(\frac{g}{L}\right)^{0.0856}$	$k = 0.3290 \cdot \frac{1}{h} \cdot \left(\frac{g}{L}\right)^{0.3495}$
$n = 1.1627$	$n = 0.9144$	$n = 0.6506$

Table 2
Converted rate constants and orders of reaction (h = hour, g = gram, L = liter).

120 °C	140 °C	180 °C
$k = 6.1908 \cdot \frac{1}{h} \cdot \left(\frac{L}{g}\right)^{0.1627}$	$k = 5.0627 \cdot \frac{1}{h} \cdot \left(\frac{g}{L}\right)^{0.0856}$	$k = 2.2813 \cdot \frac{1}{h} \cdot \left(\frac{g}{L}\right)^{0.3495}$
$n = 1.1627$	$n = 0.9144$	$n = 0.6506$

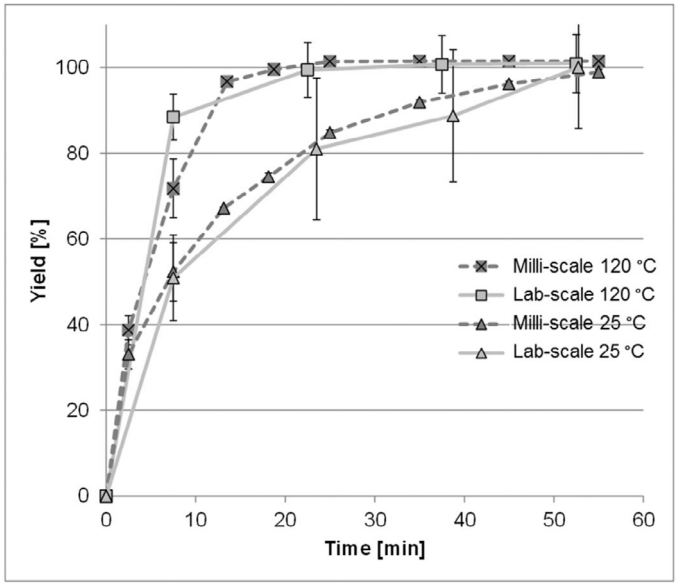

Fig. 7. Results of scale-up experiments in comparison to the milli-scale device.

Because the samples are taken from the storage vessel and not from the extraction tube itself, stirred-tank-reactor-like pseudo-kinetics are measured, which have to be converted according to reaction technology fundamentals [23,25]. On one hand, there are relatively low concentrations of the target compound in the vessel, being the basis for the calculation of the kinetic parameters. On the other hand, the fluid's and therefore the target component's residence time is significantly longer in the storage tank compared to the extraction column, where the reaction takes place. Consequently, the measured rate constants have to be higher and thus are converted, correlating the specific residence time in the storage vessel and the extraction column by equation (14). The rate constant in the extraction column is k_{EC}, in the storage vessel k_{SV}. τ_{EC} and τ_{SV} represent the corresponding residence times.

$$k_{EC} = k_{SV} \cdot \frac{\tau_{SV}}{\tau_{EC}} \tag{14}$$

The resulting rate constants are shown in Table 2. The order of reaction remains the same for all temperatures.

A standard description for temperature dependency is the implementation of the Arrhenius equation. This approach has been discarded because of the change of reaction kinetics order with temperature.

4.1.3. Scale-up

By evaluating the results of the extraction experiments and the degradation kinetics, operating at 120 °C seems to be the most productive way for a complete extraction of 10-DAB from the yew needles in the examined temperature field. To show the validity of the method, scale-up experiments are carried out at this temperature with a 13 times larger column volume. The residence time is kept constant when scaling-up from the milli-scale device to the lab-scale device. The results are plotted in Fig. 7.

The data indicate the strong conformity between the results obtained from the milli-scale device and the lab-scale device.

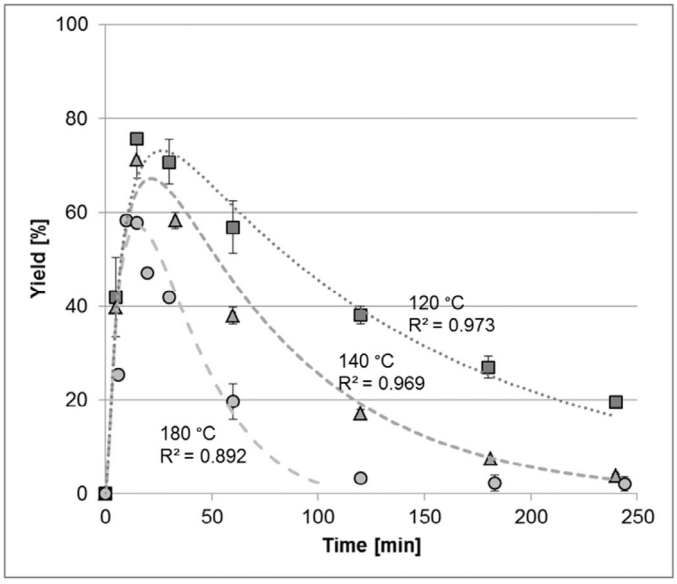

Fig. 8. Simulation results of the degradation kinetics.

4.2. Modeling and simulation

Modeling and simulation are beneficial tools for an efficient and cost saving optimization of pressurized hot water extraction. Therefore, the experimental results, as shown above, serve as a data basis for the simulation shown in this chapter.

Remark. In all of the following charts the data points represent the measurement data whereas drawn lines show simulated results. The error bars represent the standard deviation of the measurements. If there are no error bars visible they are within the symbol size of the individual data points.

4.2.1. Modeling of the degradation kinetics

Degradation is one of the most relevant parameters concerning pressurized hot water extraction. For that reason, it is crucial for process development and therefore has to be incorporated into the model. The simulation results are shown in Fig. 8. The Langmuir constant K_L is derived from the equilibrium data at ambient temperature and is assumed to be constant over temperature. Moreover, due to thermal degradation, equilibrium effects will not affect the system.

The simulation showed high sensitivity toward the order of reaction with temperature. By applying the converted reaction rate coefficients of Table 2 the order of reaction had to be adjusted by about 26% for 180 °C, only 0.1% for 140 °C and 10% for 120 °C in order to meet the experimental data best. The coefficient of determination (R^2) between simulation and experiment is 0.973 for 120 °C, 0.969 for 140 °C and 0.892 for 180 °C. The different data sets of the orders of reaction as measured and as applied in the simulation are shown in Fig. 9.

The accuracy of the determination of the kinetics parameters is absolutely sufficient, because it is only the adaption of the recycling experiments. The batch extraction curves, being the crucial point, can be simulated predictively by applying that data sets, as depicted in the following.

4.2.2. Modeling of extraction

For an industrial application the extraction curves are the primary data basis for process development and optimization. Therefore the degradation kinetics from the previous chapter are implemented and the extraction is predictively simulated. The results

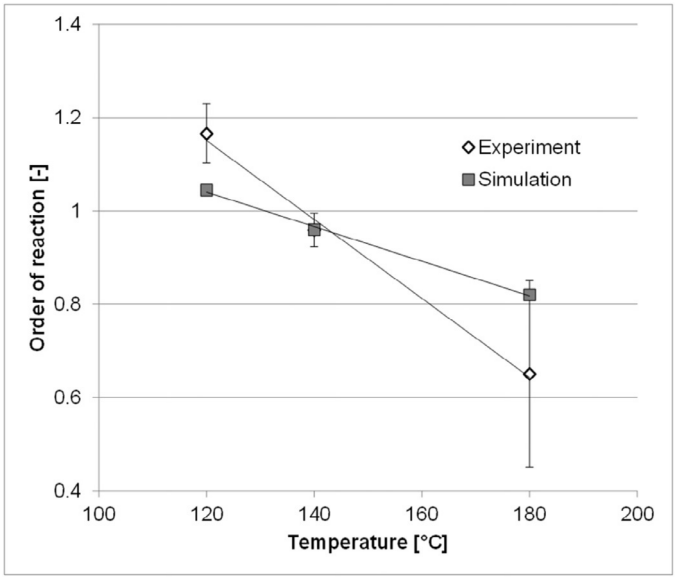

Fig. 9. Orders of reaction from experiment and simulation.

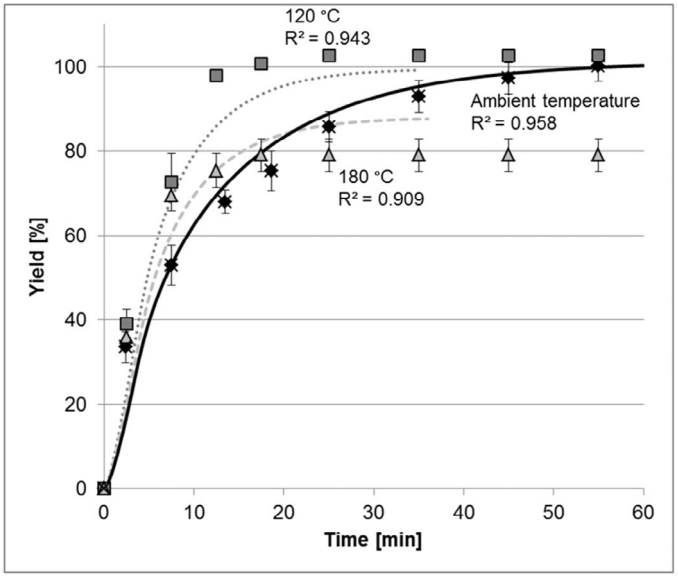

Fig. 10. Simulation results of the extraction experiments.

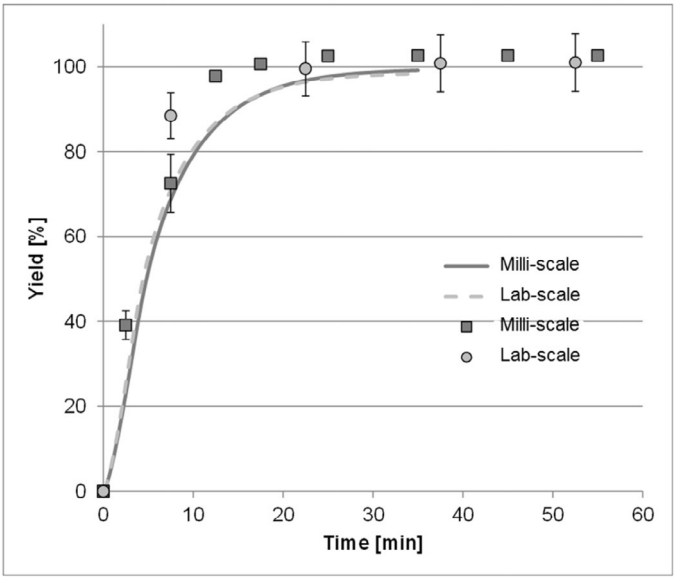

Fig. 11. Simulation results of scale-up experiments in comparison to the milli-scale device.

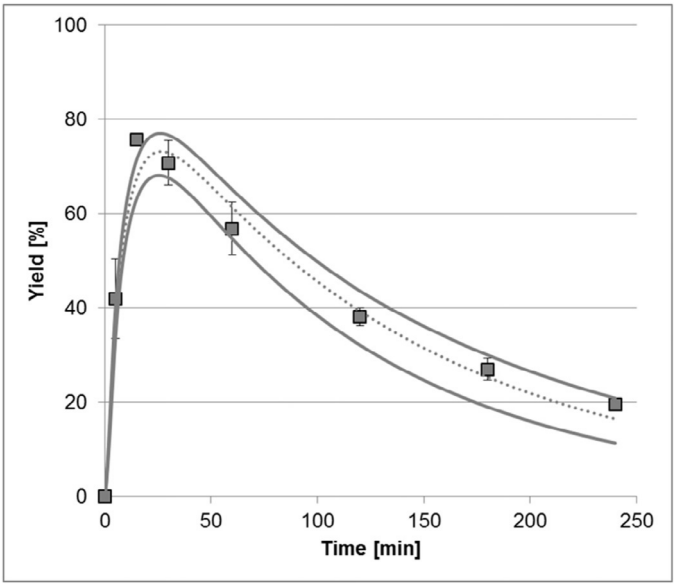

Fig. 12. Enveloping curves for the simulation at 120 °C.

are shown in Fig. 10. For ambient temperature the simulation predicts the measurements well ($R^2 = 0.958$). At 120 °C the simulation slightly overestimates the degradation ($R^2 = 0.943$), resulting in lower yield. At 180 °C the degradation is somewhat underestimated ($R^2 = 0.909$) and therefore a higher yield is predicted by the simulation.

4.2.3. Modeling of scale-up experiments

A temperature of 120 °C gave the best results in the milli-scale experiments. Therefore this temperature was used for an exemplary scale-up study. The simulation results for the milli-scale and the lab-scale devices are compared in Fig. 11. Parameters for degradation kinetics are taken from initial degradation simulations shown in Fig. 8. Other parameters like the column dimension, flux and mass of plant material are adjusted to the milli-scale. The results for the milli-scale device and the lab-scale device at the same temperature level are shown in Fig. 11. Consequently, the already mentioned overestimation of the degradation kinetics at 120 °C appears in the scale-up calculation as well. Nevertheless, there is a remarkable consistency of the two extraction curves proving the practical usefulness of the model for predictive scale-up calculations.

4.2.4. Model parameter sensitivity analysis

Process robustness is of major significance for manufacturing. The recycling experiments serve as a data basis for extraction and scale-up, thus a parameter study is performed to show the effect of inaccuracy of the model parameter determination. The parameters order of reaction, porosity of the plant material, and applied mass are changed by ±1%. Flow, initial loading of the plant material, temperature and reaction rate coefficient are changed by ±5%. The resulting enveloping curves for the experiment at 120 °C are shown in Fig. 12.

One can clearly see that the resulting curves meet the experimental data quite well even if the underlying data is distorted by measurement errors or natural fluctuations. Thus, a robust process

design is possible and deviations can be described by predictive simulations.

5. Discussion

The pressurized hot water extraction shows great potential for rapid extraction of 10-DAB from yew as an example system. PHWE by definition operates in a temperature regime above 100 °C due to the high pressure range. By operating at 120 °C the productivity can easily be increased by a factor of 3 compared to extraction at ambient temperature thus the concentration of 10-DAB is increased and there is a first bacteria count reduction in the extract. Under manufacturing aspects, of course a lower temperature of 90 °C may be an option as well, if mass transfer or solubility is efficient enough due to the higher polarity in this range.

Productivity is a sufficient key performance parameter in the process evaluation of the solid–liquid extraction step of a natural drug when operating under optimized yield conditions and within an optimized space-time-window. Final purity is reached in the subsequent purification unit operations such as liquid–liquid extraction and chromatography [16].

The calculated degradation kinetic allows predictive simulations for every investigated mode of operation including scale-up. This underlines the applicability of the developed approach. Nevertheless, the orders of reaction have to be adjusted to meet the experimental data best. The transfer of the simulation from recycling mode to real extraction shows a slight overestimation of the degradation kinetics by 2% at 120 °C, but an acceptable underestimation by 8% at 180 °C. Moreover, the order of reaction shows significant impact on the simulation result. An Arrhenius temperature dependency is not used on purpose, because of the change of the reaction kinetics order. Measurements over a wider temperature range are therefore necessary to determine this parameter more precisely in the future and control it with mass spectroscopy studies for a more fundamental comprehension [26]. At the current state of knowledge there is no satisfying explanation, since common degradation kinetics follows a reaction order of one [27]. One possible explanation could be the occurrence of equilibrium reactions which will be a focus of research with partners in the future, and their control by mass spectroscopy [26] for fundamental comprehension. The pH shift during extraction could also be a reason for the presented investigations [28,29]. For a fast and knowledge-driven process design, the developed approach is nevertheless sufficient, as shown.

All experiments, except on lab-scale, were carried out with the milli-scale device using only 1.9 g of plant material for each experiment. The small error bars shown in the charts and the good correlation between milli-scale and lab-scale device show that with minimal amounts of plant material a sufficient reproducibility and accuracy for model parameter determination is possible. Especially, in early stage of research and screening for new active pharmaceutical ingredients, with only small amounts of plants from wild collection available, this experimental set up in combination with physico-chemical (rigorous) process modeling provides a suitable tool for cost- and resource-efficient process development and scale-up studies. The relatively low operating pressure of only 11 bar compared to reports from other working groups [30,31] allows an easy and cost efficient application even in industrial, large scale operation. At the same time high yields can be achieved while using a green solvent.

6. Conclusion

The study shows the significant potential of pressurized hot water extraction, especially in the combination of experimental model parameter determination in miniaturized scale with a physico-chemical process model. The different modes of operation are simulated with slight adjustment of the parameters and meet the experimental values sufficiently well. The systematic approach shown, in combination with rigorous modeling, is suitable for scale-up studies, and therefore applicable in an industrial environment. Ongoing research is dedicated to additional applications and detailed chemical comprehension by mass spectroscopy studies. This novel process model for the description of PHWE process design and scale-up enables total process simulation studies in combination with already existing purification unit operation models [16,18–21,32,33]. Process design of natural product manufacturing processes is therefore possible also for complex mixtures with the aid of typical chemical engineering methods. Such approaches so far have been standardly applied only for smaller molecules. First industrial scale equipment for PHWE is available [34–36]. In combination with the concepts, data, and results presented this indicates the industrial potential of this new method, besides its prejudices of being complex or costly due to high temperature and pressure.

Acknowledgements

The authors would like to thank Carolin Stieg for carrying out the experiments. Special acknowledgement is extended to the ITVP laboratory and workshop team.

References

[1] F. Chemat, M.A. Vian, G. Cravotto, Green extraction of natural products: concept and principles, Int. J. Mol. Sci 13 (2012) 8615–8627.
[2] S. Both, F. Chemat, J. Strube, Extraction of polyphenols from black tea–conventional and ultrasound assisted extraction, Ultrason. Sonochem 21 (2014) 1030–1034.
[3] B. Ondruschka, W. Klemm, Überblick zur Gewinnung von Phytoextrakten, Chem. Ing. Tech 80 (2008) 803–810.
[4] F. Pena-Pereira, J. Namieśnik, Ionic liquids and deep eutectic mixtures: sustainable solvents for extraction processes, ChemSusChem 7 (2014) 1784–1800.
[5] N. Rombaut, A.-S. Tixier, A. Bily, F. Chemat, Green extraction processes of natural products as tools for biorefinery, Biofuels Bioprod. Bioref 8 (2014) 530–544.
[6] B. Tang, W. Bi, M. Tian, K.H. Row, Application of ionic liquid for extraction and separation of bioactive compounds from plants, J. Chromatogr. B. Analyt Technol Biomed Life Sci 904 (2012) 1–21.
[7] F. Chémat, J. Strube, Green Extraction of Natural Products: Theory and Practice, Wiley-VCH Verlag, Weinheim, Germany, 2015.
[8] University of Washington, Dielectric Chart. http://depts.washington.edu/eooptic/linkfiles/dielectric_chart%5B1%5D.pdf, 2015.
[9] M. Plaza, C. Turner, Pressurized hot water extraction of bioactives, Trends Anal. Chem 71 (2015) 39–54.
[10] U. Grigull, Dielektrizitätskonstante und Ionenprodukt von Wasser und Wasserdampf Sonderdruck aus BWK – Brennstoff-Wärme-Kraft 35, 1983.
[11] A. Mustafa, C. Turner, Pressurized liquid extraction as a green approach in food and herbal plants extraction: a review, Anal. Chim. Acta 703 (2011) 8–18.
[12] I. Rodriguez-Meizoso, F.R. Marin, M. Herrero, F.J. Senorans, G. Reglero, A. Cifuentes, et al., Subcritical water extraction of nutraceuticals with antioxidant activity from oregano. Chemical and functional characterization, J. Pharm. Biomed. Anal 41 (2006) 1560–1565.
[13] T. Bajer, P. Bajerová, D. Kremr, A. Eisner, K. Ventura, Central composite design of pressurised hot water extraction process for extracting capsaicinoids from chili peppers, J. Food. Compos. Anal 40 (2015) 32–38.
[14] M.B. Vázquez, L.R. Comini, J.M. Milanesio, S.N. Montoya, J.L. Cabrera, S. Bottini, et al., Pressurized hot water extraction of anthraquinones from Heterophyllaea pustulata Hook f. (Rubiaceae), J. Supercrit. Fluids 101 (2015) 170–175.
[15] C.C. Teo, S.N. Tan, J.W.H. Yong, C.S. Hew, E.S. Ong, Pressurized hot water extraction (PHWE), J. Chromatogr. A 1217 (2010) 2484–2494.
[16] M. Sixt, I. Koudous, J. Strube, Process design for integration of extraction, purification and formulation with alternative solvent concepts, C. R. Chim 19 (2016) 733–748.
[17] E. Leistner, Die Biologie der Taxane, Pharm. Unserer Zeit 34 (2005) 98–103.
[18] M. Kaßing, U. Jenelten, J. Schenk, R. Hänsch, J. Strube, Combination of rigorous and statistical modeling for process development of plant-based extractions based on mass balances and biological aspects, Chem. Eng. Technol 35 (2012) 109–132.
[19] I. Koudous, S. Both, G. Gudi, H. Schulz, J. Strube, Process design based on physicochemical properties for the example of obtaining valuable products from plant-based extracts, C. R. Chim 17 (2014) 218–231.
[20] M. Kaßing, Process Development for Plant-Based Extract Production, Shaker, Aachen, 2012.

[21] S. Both, Systematische Verfahrensentwicklung für pflanzlich basierte Produkte im regulatorischen Umfeld, Shaker, Aachen, 2015.
[22] V.D.I. Wärmeatlas, second ed., Springer, Heidelberg u.a., 2010.
[23] D.W. Green (Ed.), Perry's Chemical Engineers' Handbook, McGraw-Hill, New York, 2008 [etc.], op.
[24] S.F. Chung, C.Y. Wen, Longitudinal dispersion of liquid flowing through fixed and fluidized beds, AIChE J. 14 (1968) 857–866.
[25] M. Baerns, Technische Chemie, Wiley-VCH-Verl, Weinheim, 2006.
[26] G. Gudi, A. Krahmer, I. Koudous, J. Strube, H. Schulz, Infrared and Raman spectroscopic methods for characterization of Taxus baccata L.-Improved taxane isolation by accelerated quality control and process surveillance, Talanta 143 (2015) 42–49.
[27] O. Levenspiel, Chemical Reaction Engineering, second ed., Wiley, New York, NY, 1972.
[28] J. Tian, V.J. Stella, Degradation of paclitaxel and related compounds in aqueous solutions III: Degradation under acidic pH conditions and overall kinetics, J. Pharm. Sci 99 (2010) 1288–1298.
[29] J. Tian, V.J. Stella, Degradation of paclitaxel and related compounds in aqueous solutions I: epimerization, J. Pharm. Sci 97 (2008) 1224–1235.
[30] K. Hartonen, J. Parshintsev, K. Sandberg, E. Bergelin, L. Nisula, M.-L. Riekkola, Isolation of flavonoids from aspen knotwood by pressurized hot water extraction and comparison with other extraction techniques, Talanta 74 (2007) 32–38.
[31] C. Rodríguez-Pérez, J. Mendiola, R. Quirantes-Piné, E. Ibáñez, A. Segura–Carretero, Green downstream processing using supercritical carbon dioxide, CO2-expanded ethanol and pressurized hot water extractions for recovering bioactive compounds from Moringa oleifera leaves, J. Supercrit. Fluids 116 (2016) 90–100.
[32] E. Ndocko Ndocko, W. Bäcker, J. Strube, Process design method for manufacturing of natural compounds and related molecules, Sep. Sci. Technol 43 (2008) 642–670.
[33] S. Both, J. Eggersglüß, A. Lehnberger, T. Schulz, T. Schulze, J. Strube, Optimizing established processes like sugar extraction from sugar beets – design of experiments versus physicochemical modeling, Chem. Eng. Technol 36 (2013) 2125–2136.
[34] B. Lightburn, G. Mazza, An introduction to the green, clean and economical Mazza Extraction Technology, Turin, 2016.
[35] G. Mazza, C. Pronyk, Pressurized low polarity water extraction apparatus and methods of use, 2014.
[36] Mazza Innovation Ltd., Homepage of Mazza Innovation. http://mazzainnovation.com/, 2015.